Inf Syst E-Bus Manage
DOI 10.1007/s10257-014-0261-4

ORIGINAL ARTICLE

A novel information technology of load events detection for the energy management information systems

Hsueh-Hsien Chang · Ching-Lung Lin

Received: 22 November 2013 / Revised: 29 August 2014 / Accepted: 13 September 2014

Abstract Coordinating economic load demand response (ELDR) strategy with energy efficiency and information technology (IT) of e-business management multiplies the reduction in electricity usage. The steady-state power signatures (PS) contain plenty of information needed for detecting state transition and aging of loads. On the other hand, adopting the values of PS directly has the drawbacks of taking a longer time and much memory for the datasets of energy management information system (EMIS). To effectively reduce the number of PS representing load state transition and aging signals, a feature extraction technique of the PS in the EMIS, Hellinger distance, is proposed in this paper. The high success rates of identifying state transition and aging of loads from the back-propagation artificial neural network (BP-ANN) have been proved via experiments to be feasible in load operations of EMIS applications.

Keywords Energy management information system (EMIS) · Load event detection · Economic load demand response (ELDR) · Information technology (IT) · Data mining

H.-H. Chang (✉)
Department of Electronic Engineering, Jin Wen University of Science and Technology, No. 99, Anzhong Rd., Xindian Dist., New Taipei City 23154, Taiwan, ROC
e-mail: h.h.johnson.chang@gmail.com; sschang@just.edu.tw

C.-L. Lin
Department of Electrical Engineering, Ming Hsin University of Science and Technology, Hsin-Chu, Taiwan, ROC
e-mail: cll@must.edu.tw

Published online: 01 October 2014

1 Introduction

Today it is normal for buildings to collect huge amounts of real-time energy use data from energy monitoring systems, including programmable logic controller (PLC), supervisory control and data acquisition (SCADA) system, etc. However, unless this captured data is shared and analyzed in a regular and efficient way to identify problems and provide solutions, this mass of data is merely overloaded with information.

An energy management information system (EMIS) is a performance management system that enables individuals and organizations to plan, make decisions and take effective action to manage energy use and costs. An EMIS can be characterized by its deliverables, features, elements and support. Deliverables include the early detection of poor performance, support for decision making and effective energy reporting. Features of an EMIS include the storage of data in a usable format, the calculation of effective targets for energy use, and comparison of actual consumption with these targets. Elements include sensors, energy meters, hardware and software. Essential support includes management commitment, the allocation of responsibility, procedures, training, resources and regular audits (Hooke et al. 2004). Figure 1 shows a typical EMIS in a building system. Single-phase two-wire and single-phase three-wire systems are generally used to run a typical residential or office building system.

Economic load demand response (ELDR) program uses monitoring and control devices to manage what business takes from the power grid during expensive high demand and high energy use periods. With ELDR, businesses can save money by using less energy or shifting electric load during high demand and high cost periods. Over the past two decades, there have been many techniques proposed on ELDR for establishing various energy consumption managements of the EMIS (Hou et al. 2006; Verdu et al. 2006; Timbus et al. 2009; Lisovich et al. 2010; Byun et al. 2011; Silva et al. 2011; Chan et al. 2012; Hernandez et al. 2013). Aman et al. (2013) provided a comprehensive review of the literatures for the EMIS. In addition, they presented a survey of the state of the art in energy management (EM) systems, applications, and frameworks. Hou et al. (2006) proposed a data mining method, combining a rough set approach and an artificial neural network (ANN), to detect and diagnose sensor faults based on the past running performance in the heating, ventilating, and air conditioning (HVAC) systems. Timbus et al. (2009) introduced the communication standards International Electrotechnical Commission (IEC) 61400-25, IEC 61850, and their extensions of distributed generators (DGs) for active management of distributed energy resources (DER) to optimize the scheduling of the production of wind energy and combined heat and power (CHP) systems while managing capacity constraints and minimizing the total operational cost. Byun et al. (2011) proposed a smart energy distribution and management system (SEDMS) to monitor information about power consumption, a user's situation and surroundings as well as controls appliances using dynamic patterns based intelligent services and adaptive demand management to make the distribution and consumer more energy efficient and intelligent. Accordingly, the results showed that a reduction of the service response time and the power

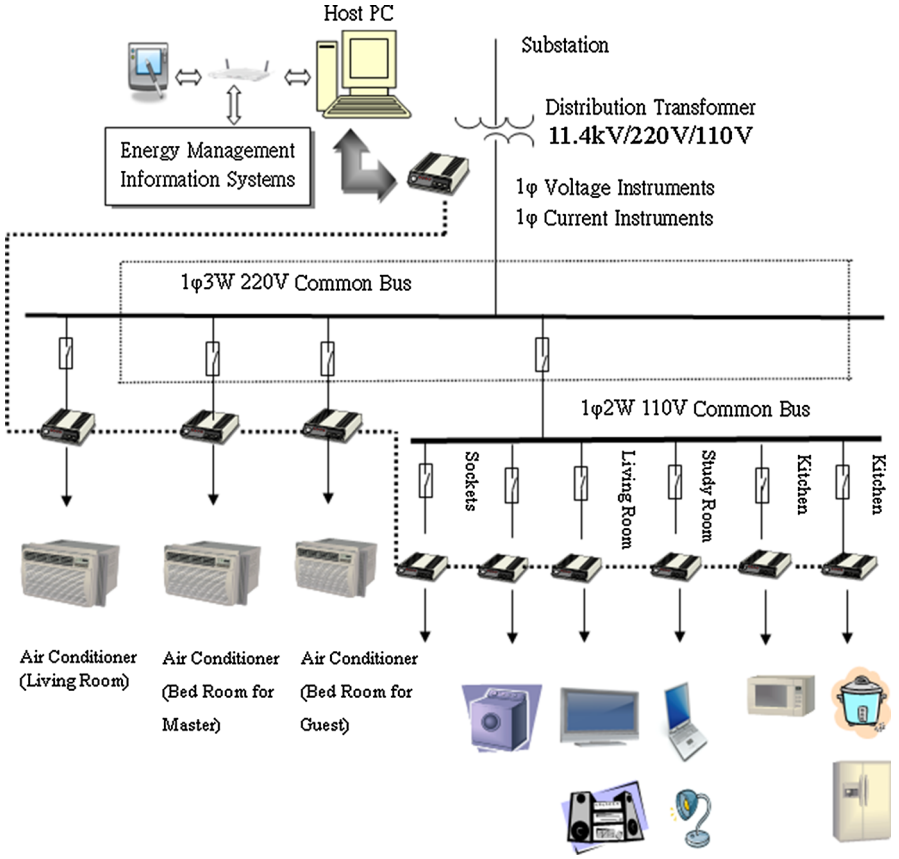

Fig. 1 Energy management information systems in a building system

consumption are about 45.6 % and 9–17 %, respectively. Silva et al. (2011) presented a novel data mining framework for the exploration and extraction of actionable knowledge from data of energy consumption analysis generated by electricity meters. In addition, the proposed framework can incorporate functionality for interim summarization and incremental analysis using intelligent techniques. Chan et al. (2012) introduced a signal processing community concept of smart grids on the problems of price/load forecasting and demand response management (DRM) and optimization.

For the load detection, a lot of papers have been published to improve the performance of recognition for the power system. For example, Bernstein and Brancato (1993) described the typical mechanism of aging for each class of utility equipment and analyze the limits of any multifactor aging relationship's ability to predict a component's life. Su (2011) proposed a two-stage load estimator algorithm that combines typical load characteristics and state estimation theory is developed to provide the injected power at load buses in the network at a sound accuracy with relatively few real measurements. For the home appliances, Lall et al. (2011)

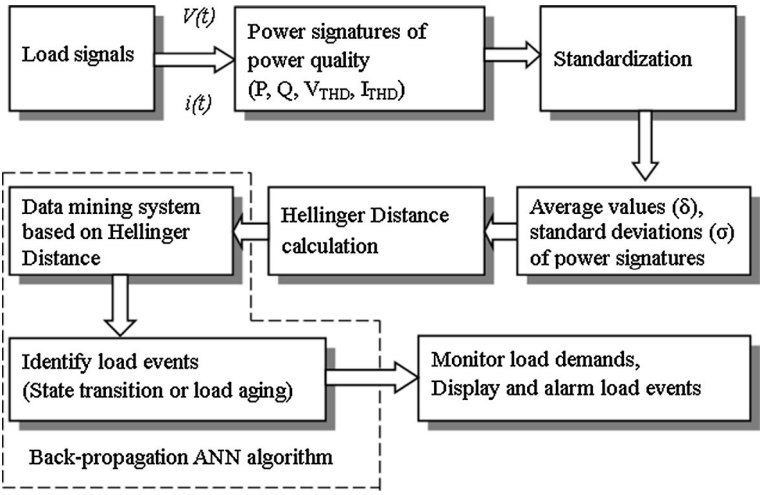

Fig. 2 Block diagram of a load event identification system

presented a mathematical approach to calculate the prior damage in electronics subjected to cyclic and isothermal thermo-mechanical loads. In the paper, the prognostic parameters and proposed methodology enabled tracking of damage progression and prior damage assessment and resides in the pre-failure-space of the electronic system. Redpath and Pocs (2007) provided a list of the elements of the microcontroller for home users that must be monitored and tested, the type of faults to be detected, and recommended tests to help customers comply with the requirements of Category B of IEC60730 and Class 1 of UL 1998. Goumas et al. (2002) presented a method, discrete wavelet transform (DWT) in conjunction with statistical digital signal processing techniques, for extracting features in the wavelet domain and uses them for classification of washing machines vibration transient signals.

This paper presents a novel event identification of ELDR system consisting of two models as shown in Fig. 2. First, the power signatures (PS) of power system proposing techniques and the standardization of PS are utilized to extract the energy distribution features of the load state transition and aging load for the individual event at different times. Second, the Hellinger distance is employed to classify load statuses in state transition and aging of loads according to the detailed energy distribution. By using the data mining model of Hellinger distance, the number of power features can be reduced without losing its property.

Taking the data collected from EMIS and analyzing the data using data mining techniques are not very new. However, the researches of studying state transition and aging of loads are valuable and innovative ideas for ELDR of the safety and quality of intelligent buildings in EMIS. The accurate rate and computation requirement of the proposed method were measured and implemented by real case studies. Accordingly, these results showed that the proposed method can analyze the power demand efficiently, thus enhance the performance of the EMIS and efficiently manage energy use and costs.

The ELDR program allows end-users to get paid for reducing electricity demand during high-priced hours. Participants receive the same price as generators and also realize savings on their electricity bills. On the one hand, the ELDR algorithm uses cluster analysis to detect the events of the load state transition and aging load in the EMIS, and the proposed method can combine with information technology (IT) to employ in e-business engineering. For examples, decision support of intelligent buildings for e-business, applications of predictive load modeling to e-business, real-time ELDR analytics for e-business, green business, data and knowledge management for e-Business, and etc. Accordingly, the ELDR program can extensively identify the real-time state change of energy market and monitor aging business model for other service engineering.

In the future, the EMIS can cope with a large volume of data to generate an effective and real time appliance level advice on load profiles and energy consumptions (Chao et al. 2012). The system may use an approach based on functional data services in a service-oriented architecture (SOA) or service-oriented applications, integration and collaboration (SOAIC) to deal with the challenge of processing a large volume of data in real time. The service identification system can determine which services are appropriate to be implemented by supporting the SOA adoption to hand many perspectives of the services for the EMIS (Huergo et al. 2014; Huber et al. 2014).

This paper is organized as follows. The research motivation, research purposes, and relative papers reviews are addressed and described in Sect. 1. The proposed methods of the paper are introduced in Sect. 2, which includes Hellinger distance, standardization, ANNs, and PS of steady state; for examples, real power, reactive power, and the total harmonic distortions of voltage and current. Based on the data mining techniques, a series of ELDR analyses for detecting events of the load state transition and aging load are implemented for real case studies in Sect. 3. The discussions are addressed in Sect. 4 to explain the results of experiments. Finally, the conclusion is stated in Sect. 5.

2 Proposed methods

The block diagram in Fig. 2 includes the algorithms of PS of power system, i.e. real power (P), reactive power (Q), total harmonic distortions of voltage (V_{THD}), and total harmonic distortions of current (I_{THD}), the processes of the standardization technique, extraction of the features from statistics of PS, data mining system based on the Hellinger distance, the identification of load events, i.e. state transition or aging load, and load demand monitoring and events alarm.

2.1 Power signatures

The current and voltage consumed for a periodically nonlinear load can be represented by a Fourier series expansion (FSE). The appropriate coefficients corresponding to the current and voltage in each harmonic are extracted from the results of FSE. The number of terms represented by the expansion determines the

dimension of the feature vector. The real power and reactive power can be computed by

$$P = \sum_{n=0}^{N} P_n = V_0 I_0 + \sum_{n=1}^{N} \frac{1}{2} V_n I_n \cos(\theta_{V_n} - \theta_{I_n}) \tag{1}$$

and

$$Q = \sum_{n=1}^{N} Q_n = \sum_{n=1}^{N} \frac{1}{2} V_n I_n \sin(\theta_{V_n} - \theta_{I_n}) \tag{2}$$

where n is the harmonic number; V_0 and I_0 are the average voltage and average current, respectively; V_n and I_n are the effective nth harmonic components of the voltage and current; θ_{V_n} and θ_{I_n} represent the phase angles of nth harmonic components of the voltage and current, respectively. The total harmonic distortions of voltage and current can be computed by (3) and (4), respectively.

$$\mathrm{V_{THD}}\% = \frac{\sqrt{|\mathrm{V_2}|^2+|\mathrm{V_3}|^2+|\mathrm{V_4}|^2+\cdots}}{|\mathrm{V_1}|} \times 100\% \tag{3}$$

$$\mathrm{I_{THD}}\% = \frac{\sqrt{|\mathrm{I_2}|^2+|\mathrm{I_3}|^2+|\mathrm{I_4}|^2+\cdots}}{|\mathrm{I_1}|} \times 100\% \tag{4}$$

2.2 Standardization

Data expressions can be made more efficient if certain preprocessing steps are performed on the data mining system. Before mining, it is often useful to scale the power signature inputs so that they always fall within a specified range. The approach for scaling inputs is to normalize the mean and standard deviation of the training set, normalizing the inputs so that they will have zero mean and unity standard deviation. These can be computed by

$$P_n = (P - \mu_p)/\sigma_p \tag{5}$$

$$Q_n = (Q - \mu_Q)/\sigma_Q \tag{6}$$

$$V_{THDn} = (V_{THD} - \mu_{V_{THD}})/\sigma_{V_{THD}} \tag{7}$$

$$I_{THDn} = (I_{THD} - \mu_{I_{THD}})/\sigma_{I_{THD}} \tag{8}$$

where the matrices P, Q, V_{THD}, *and* I_{THD} are the original power signature inputs of real power, reactive power, and the total harmonic distortions of voltage and current, respectively, the matrices P_n, Q_n, V_{THDn}, *and* I_{THDn} represent the normalized power signature inputs of P, Q, V_{THD} and I_{THD}, respectively. The vectors μ and σ contain the mean and standard deviations of the original power signature inputs, respectively.

2.3 Hellinger distances

The squared Hellinger distance is used to quantify the similarity between two normal probability distributions in probability and statistics. The Hellinger distance is expressed in terms of the Hellinger integral, which was first developed in the 1909 by Ernst Hellinger (Hellinger 1909; Nikulin 2001). For two discrete probability distributions $I = (i_1, i_2, i_3, \cdots, i_N)$ and $J = (j_1, j_2, j_3, \cdots, j_N)$, their squared Hellinger distance is defined as

$$\begin{aligned} d_H^2(I,J) &= \frac{1}{2}\sum_{n=1}^{N}(\sqrt{i_n} - \sqrt{j_n})^2 \\ &= \frac{1}{2}\sum_{n=1}^{N}(i_n + j_n - 2\sqrt{i_n j_n}) \end{aligned} \tag{9}$$

where n is a sampling time point, for $n = 1, 2, \ldots, N$, and N is the number of sampling points. Set

$$\sum_{n=1}^{N} i_n = 1; \sum_{n=1}^{N} j_n = 1 \tag{10}$$

then (9) is resulted

$$d_H^2(I,J) = \frac{1}{2}\left(2 - 2\sum_{n=1}^{N}\sqrt{i_n j_n}\right) = 1 - \sum_{n=1}^{N}\sqrt{i_n j_n} \tag{11}$$

where $0 \le d_H^2 \le 1$, the $d_H^2 = 0$ when I and J are similar; otherwise, the squared Hellinger distance is equal to one when I and J are different from each other i.e. $d_H^2 = 1$. The normal distribution is a continuous probability distribution. The squared Hellinger distance can be expressed as

$$H^2(I,J) = 1 - \sqrt{\frac{2\sigma_i\sigma_j}{\sigma_i^2 + \sigma_j^2}} e^{-\frac{1}{4}\frac{(\mu_i^2 - \mu_j^2)^2}{\sigma_i^2 + \sigma_j^2}} \tag{12}$$

Here, two normal distributions I and J are defined as follows:

$$I \sim N(\mu_i, \sigma_i^2), J \sim N(\mu_j, \sigma_j^2) \tag{13}$$

where the parameter μ in this formula is the mean of the distribution. The parameter σ is its standard deviation; its variance is therefore σ^2. A random variable with a Gaussian distribution is said to be normally distributed and is called a normal deviation.

The Hellinger distance is closely related to the total variation distance; for example, both distances define the same topology of the space of probability measures, but it has several technical advantages derived from properties of inner products. Hellinger distances are very well suited for the study of similarity of two

normal probability distributions. In this paper, the squared Hellinger distance is employed to extract PS for load events i.e. state transition and aging load.

2.4 Artificial neural networks

Pattern classifiers partition a multidimensional space into decision regions that indicate the class to which any input belongs (Norford and Leeb 1996).

2.4.1 Training algorithms and fitness function

Over-fitting is a typical problem that occurs during ANN training. Bayesian regularization (mean square error, MSE) typically provides better generalization performance than early stopping because it does not require a validation dataset to be separated from the training dataset. In other words, the input training data uses all training datasets. This advantage is particularly important when the available dataset is small.

The typical fitness function used for training a feed-forward neural network is the mean sum of squares of network errors, also called MSE, which is the average squared error between network outputs and desired outputs.

$$MSE(l) = \frac{1}{2}\sum_{j \in C}(t_j(l) - a_j(l))^2 \tag{14}$$

where the variable $t_j(l)$ is the desired output for the lth iteration at node j, and variable $a_j(l)$ is the network output for the lth iteration at node j.

2.4.2 Multi-layer feed-forward neural network

Most back-propagation artificial neural network (BP-ANN) applications utilize single- or multilayer perceptron networks by using gradient-descent training methods combined with learning via back propagation. These multi-layer perceptrons can be trained under supervision using analytical functions to activate network nodes ("neurons") and by applying a backward error-propagation algorithm to update interconnecting weights and thresholds until a sufficient recognition capability is achieved. A trainable classifier uses the BP classifier for a multi-layer feed-forward neural network (MFNN) in this study. "Classification" in this context is a mapping from a feature space to a set of class labels, which are the names of loads.

A supervised MFNN is generally divided into three layers: input, hidden, and output layers. These neurons are connected by links with weights that are selected to meet the desired relationship between input and output neurons. The MFNN is utilized to identify aging loads in the EMIS system. The input, output, and hidden layers of the BP-ANN are as follows:

(a) Input layer: PS information, the number of input neurons is the sum of the number of neurons in the the mean and standard deviation of the training set of PS.

(b) Output layer: the number of output neurons is the same as the number of load statuses identified. Each binary bit serves as a load indicator for load status (two status) in the case of state transition, and for new/old status in the case of aging load, respectively.
(c) Hidden layer: only one hidden layer is used in this study. Some heuristics have been developed that can determine the number of neurons in a hidden layer (Hong and Chen 2007). The common number of neurons in a hidden layer is the sum of the number of neurons in an input layer and that in an output layer.

3 Experimental results

3.1 Case study environment

In case studies, the EMIS monitors voltage and current waveforms in a single-phase electrical service entry (ESE) powering a collection of loads representative of the major loads in a residential building. The data mining algorithm in the EMIS identifies loads with steady-state signatures operating on a 110-V common bus. These loads include an electric rice cooker and a refrigerator.

Experimental datasets were generated by preprocessing the data on the voltage and current waveforms of the load. Each final sample consists of 80 data samples and 96 data samples obtained over a period of 40 min for an electric rice cooker and a period of one day for a refrigerator, respectively. Each example of the power feature includes a voltage variation from -20 to $+20$ % at 1 % intervals, yielding forty-one examples of power feature for each scenario. A data mining simulation program was designed using MATLAB. The program was run to identify load on an ASUS PC with a 2.4 GHz Intel Quad Core i7- 4700HQ CPU.

Each entry in the BP-ANN represents 10 different trials, and each trial uses random initial weights. In each case, the network is trained until the MSE is less than 0.0001 or the number of iterations reaches 5000.

3.2 Results

3.2.1 Case study 1, state transition

In case study 1, the EMIS monitors the state transition of an electric rice cooker and a refrigerator in a single-phase ESE powering a collection of loads representative of the major loads in a residential building.

Figures 3, 4 show the state transition of an electric rice cooker and a refrigerator on the PS of P and Q, respectively. The clusters of the load state transition are clear; however the load is the electric rice cooker or refrigerator. The variety of power of a refrigerator is bigger than that of an electric rice cooker; however the compressor of refrigerator is working or without working.

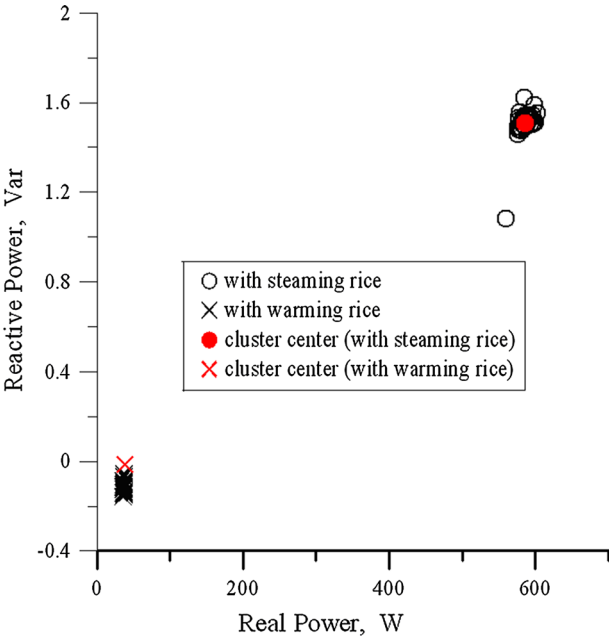

Fig. 3 State transition of an electric rice cooker

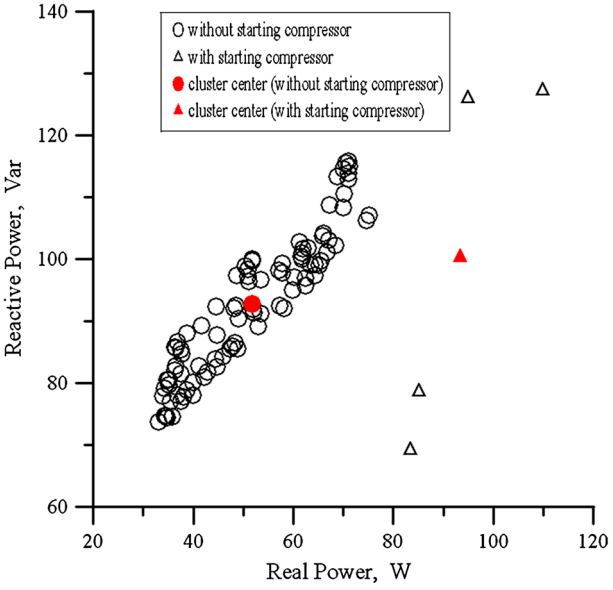

Fig. 4 State transition of a refrigerator

Table 1 Results of feature extraction for an electric rice cooker in case study 1

States	P (W)	Q (Var)	V_{THD} (%)	I_{THD} (%)
Steam				
μ	585.8242	1.5073	5.1467	0.3280
σ	7.9700	0.2045	0.0225	0.0040
Warm				
μ	36.2723	0.1081	5.9911	0.01915
σ	0.0120	0.0382	0.0615	0.0007
Hellinger distance	1	1	1	1

Table 2 Results of state transition identification for an electric rice cooker in case study 1

Features	PQ	$PQV_{THD}I_{THD}$
Recognition accuracy in training (%)	100	100
Recognition accuracy in test (%)	99.39025	99.2683
Training time (s)	0.66525	1.09739
Test time (s)	0.01661	0.0198

Table 3 Results of feature extraction for a refrigerator in case study 1

States	P (W)	Q (Var)	V_{THD} (%)	I_{THD} (%)
Without compressor				
μ	51.0903	92.0950	2.3973	0.3043
σ	11.9746	10.4281	0.0982	0.0129
With compressor				
μ	91.8347	102.4634	2.38049	0.2972
σ	10.0658	26.8450	0.0978	0.0184
Hellinger distance	1	1	0.0806	0.0388

Table 1 shows that the feature extraction results of state transition for an electric rice cooker. The values of mean, standard deviation, and Hellinger distance are calculated for different PS when an electric rice cooker works in steaming status or in warming status. In the results, the values of mean and standard deviation of P, Q, V_{THD}, and I_{THD} are extracted to be the input neurons of BP-ANN. Table 2 shows the identification results of state transition for an electric rice cooker. From the results, the state transition can be identified by the steady-state PS extracted by the proposed method. Regarding the computation time, the time of training for the proposed features with PQ is smaller than that of the features with $PQV_{THD}I_{THD}$.

Table 3 shows that the feature extraction results of state transition for a refrigerator. The values of mean, standard deviation, and Hellinger distance are also calculated for different PS when a refrigerator works with compressor and without compressor. In the results, the values of mean and standard deviation of P and Q are extracted to be the input neurons of BP-ANN. Table 4 shows that values for the

Table 4 Results of state transition identification for a refrigerator in case study 1

Features	PQ	$PQV_{THD}I_{THD}$
Recognition accuracy in training (%)	100	100
Recognition accuracy in test (%)	94.9997	64.28572
Training time (s)	0.32303	0.3127
Test Time (s)	0.00353	0.00367

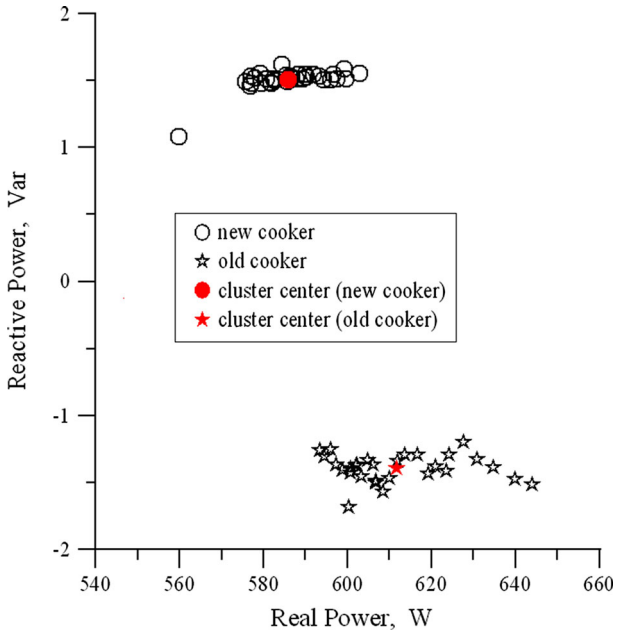

Fig. 5 Aging load patterns of an electric rice cooker in steaming operation

training accuracy of state transition identification are all 100 % for features with the proposed PQ and $PQV_{THD}I_{THD}$ features for a refrigerator. Furthermore, the test accuracy of load identification is near 95 % for proposed PQ features. However, the identification rate of test is the highest for the proposed features, which use P and Q as the PS. The PQ features, in combination with V_{THD} and I_{THD} features, cannot improve the recognition accuracy. In terms of the computation time, the proposed features PQ, in general takes same time for training when compared to others.

3.2.2 Case study 2, aging load

In case study 2, the EMIS monitors aging load of an old electric rice cooker made in 1998 and a new electric rice cooker made in 2012 in a single-phase ESE powering a collection of loads representative of the major loads in the laboratory.

Figures 5, 6 show the aging load of the electric rice cooker when it works in steaming operation and warming operation for the PS of P and Q, respectively. The

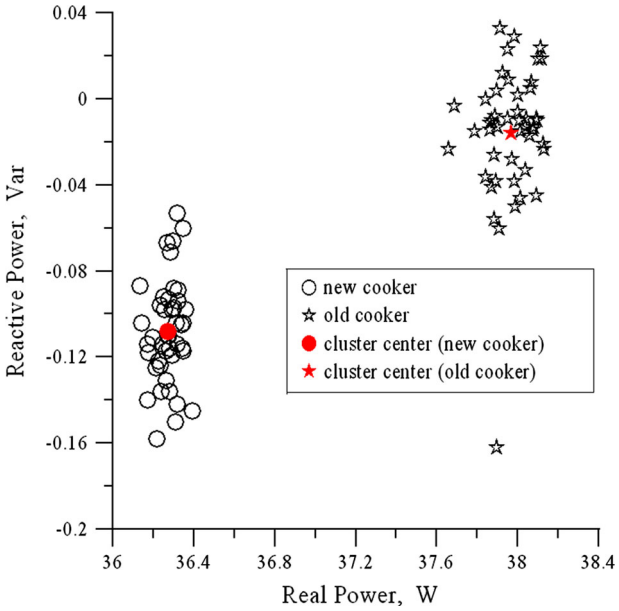

Fig. 6 Aging load patterns of an electric rice cooker in warming operation

clusters of aging load are very clear; however the load works in steaming and warming. Furthermore, the power consumptions of the old electric rice cooker are bigger than that of the new one regardless of steaming and warming operations.

Table 5 shows that the feature extraction results of aging load when the electric rice cooker works in steaming operation. The values of mean, standard deviation, and Hellinger distance are calculated for different PS. In the results, the values of mean and standard deviation of P, V_{THD}, or I_{THD} are extracted to be the input neurons of BP-ANN. The reactive power of the electric rice cooker is very small because the electric rice cooker is a resistive load. Nevertheless, the variation of reactive power in the aging load is not distinct easily from the proposed method. Table 6 shows that the recognition accuracy of aging load identification in steaming operation in training and test for features with P and $PV_{THD}I_{THD}$ are 100 % and above 97 %, respectively. However, the test recognition accuracy of aging load identification is only 78.29 % for feature with Q. The test recognition for this load in steaming operation is quite low when using only feature with Q. Regarding the computation time, the time of training for the proposed features is shorter than that of the feature with Q.

Table 7 shows that the feature extraction results of aging load when the electric rice cooker works in warming operation. The values of mean, standard deviation, and Hellinger distance are also calculated for different PS. From the results, the values of mean and standard deviation of P, V_{THD}, or I_{THD} are also extracted to be the input neurons of BP-ANN like as previous case study. The reactive power of the electric rice cooker cannot be employed to identify the aging load of the electric rice

Table 5 Results of feature extraction for an electric rice cooker during steaming in case study 2

States	P (W)	Q (Var)	V_{THD} (%)	I_{THD} (%)
New				
μ	585.8242	1.5073	1.9332	0.1230
σ	7.9700	0.2045	0.0489	0.0029
Old				
μ	611.6456	1.3884	4.6292	0.2953
σ	4.8918	0.2984	0.0477	0.0029
Hellinger distance	1	0.2301	1	1

Table 6 Results of aging load identification for an electric rice cooker during steaming in case study 2

Features	P	Q	$PV_{THD}I_{THD}$
Recognition accuracy in training (%)	100	84.34148	100
Recognition accuracy in test (%)	100	78.29269	97.80488
Training time (s)	0.33186	14.84772	0.34113
Test time (s)	0.00363	0.00356	0.00369

Table 7 Results of feature extraction for an electric rice cooker during warming in case study 2

States	P(W)	Q(Var)	V_{THD}(%)	I_{THD}(%)
New				
μ	36.2723	0.1081	5.9911	0.01915
σ	0.0120	0.0382	0.0615	0.0007
Old				
μ	37.9649	0.0157	5.8787	0.0210
σ	0.1492	0.0127	0.0297	0
Hellinger distance	1	0.2409	1	1

Table 8 Results of aging load identification for an electric rice cooker during warming in case study 2

Features	P	Q	$PV_{THD}I_{THD}$
Recognition accuracy in training (%)	100	79.26832	100
Recognition accuracy in test (%)	100	52.43905	97.12
Training time (s)	0.32056	15.54502	0.32906
Test time (s)	0.00410	0.00406	0.00413

cooker. The reason for this is the same as that for the previous explanations. Accordingly, the variation of reactive power in the aging load is not distinguished by using the proposed method. Table 8 shows that the recognition accuracy of aging load identification in warming operation in training and test are 100 % and above

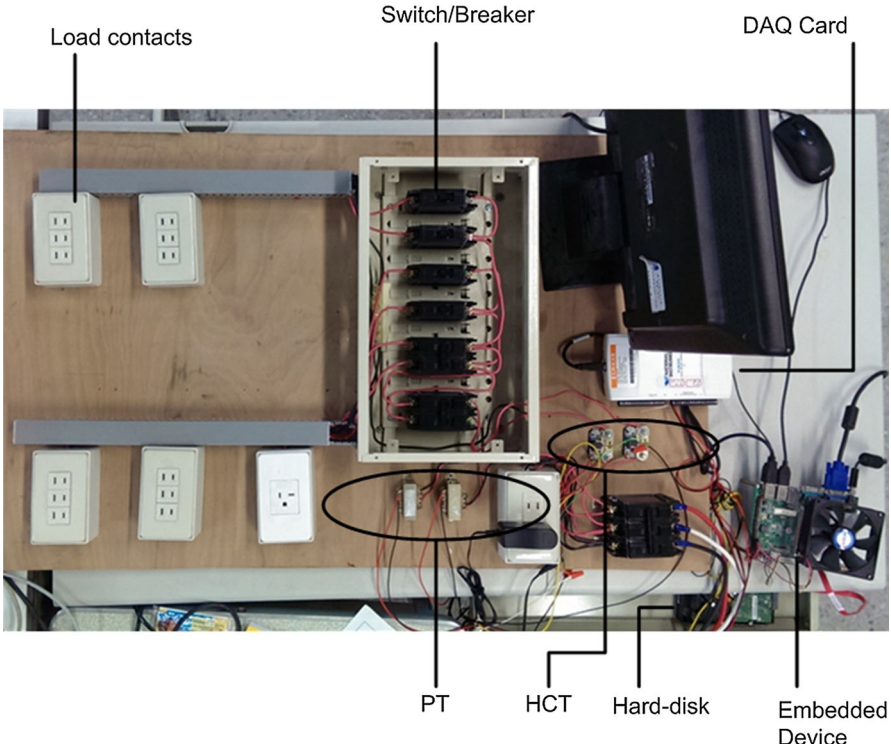

Fig. 7 Experimental platform for EMIS based on the embedded system

97 % for features with P and $PV_{THD}I_{THD}$, respectively. However, the train and test recognition accuracies of aging load identification are 79.26 % and 52.43 % for feature with Q, respectively. The test recognition for those loads in warming operation is also quite low when using only feature with Q. In computation requirements, the time of training for the power signature with Q is higher than that of the power signature with others.

3.2.3 Case study 3, EMIS in the residential buildings

The EMIS system in this case is built in the household model to monitor voltage and current waveforms in an unbalanced single-phase three-wire 220 V/110 V ESE powering a collection of loads representing the major load classes in a residential building. Figure 7 shows a typical EMIS experimental system.

This study uses potential transformers (PTs) and current transformers (CTs). PTs are used to measure voltage. These PTs are traditional PTs with normal 110 V/6 V ratio. In this research, Hall sensors are used to replace traditional iron cored CTs. This transformer is called Hall Current Transformer (HCT). The embedded system is a Portwell PQ7-C100XL with Intel Atom processor. The system is equipped with a processor, USB Inputs/Outputs, memory and single Ethernet controller.

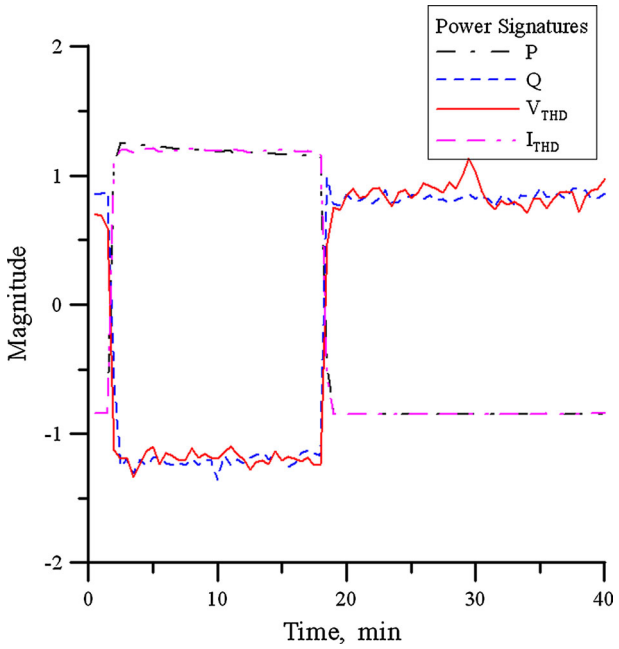

Fig. 8 Power signature analyses of an electric rice cooker

Figure 8 shows steady-state power signature waveforms of an electric rice cooker. Each sample is a mean value of the P and Q over a period of 30 s and an instantaneous value of the V_{THD} and I_{THD} at 30 s. The values of these steady-state signatures are not stationary when the electric rice cooker is used for a long time because of operation temperature (Chang 2012). In addition, there is a state transition of PS from steaming status to warming status.

Figure 9 shows steady-state power signature waveforms of a refrigerator. Each sample is a mean value of the P and Q over a period of 15 min and an instantaneous value of the V_{THD} and I_{THD} at 15 min. The values of these steady-state signatures are also not stationary when the refrigerator is operated for a long time. Moreover, there is a state transition of PS during compressor operation.

Figure 10 shows aging load analyses of the new and old electric rice cookers when the cookers work in state transition operation. Each sample is a standardized value of the P over a period of 22.5 min. The times of state transition of the old and new electric rice cookers are at 11:38:00 and 11:42:30, respectively. In load disaggregation, the time of the state transition for the old electric rice cooker is earlier than that of the new one. Obviously the P value of the old electric rice cooker is higher than that of the new one.

Figure 11 shows aging load analyses of the new and old electric rice cookers when the cookers work in warming operation. Each sample is a standardized value of the P over a period of 12.5 min. In load disaggregation, the P values of the old electric rice cooker vary greatly during warming operation. In addition, it is difficult

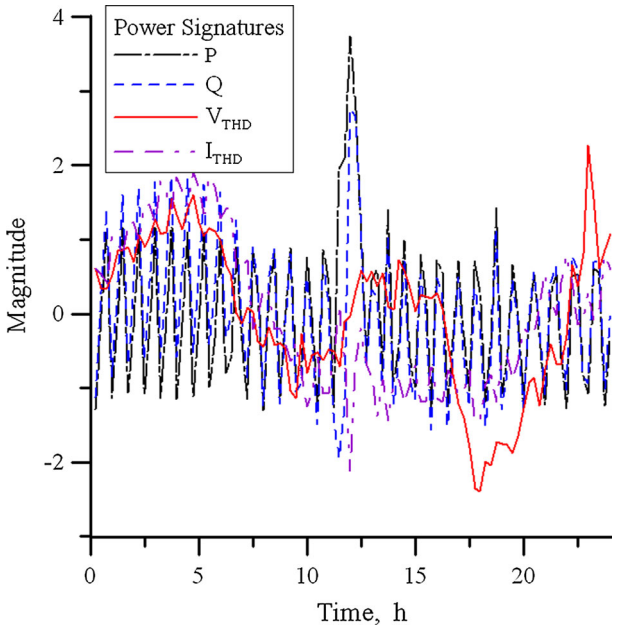

Fig. 9 Power signature analyses of a refrigerator

to analyze the aging load because the power consumption is very low, regardless whether the electric rice cooker is new or old.

4 Discussion

In this paper, the electric rice cooker and the refrigerator were chosen as the experimental examples to verify the performance of the EMIS. The loads, the electric rice cooker and the refrigerator, are often basic electric appliances for every day in the home. However, the representatives of two examples have strong relevance with the research topic of the load state transition and aging load for the smart building.

An appliance may have numerous load representations and a load may be determined by various physical components. For example, an electric rice cooker has only one load, a heater, but has different physical components for steaming and warming operations. A refrigerator has two loads, a fan motor and a compressor, have different physical components for cold storage and freezing operations. For the state transition in case study 1, the state transition of the appliances can be identified basically by the proposed method for steady-state PS of P and Q. The state transition identification of refrigerator is irrelevant to harmonics of the load; steady-state PS of V_{THD} and I_{THD} are difficult to identify the state transition by proposed method for the refrigerator.

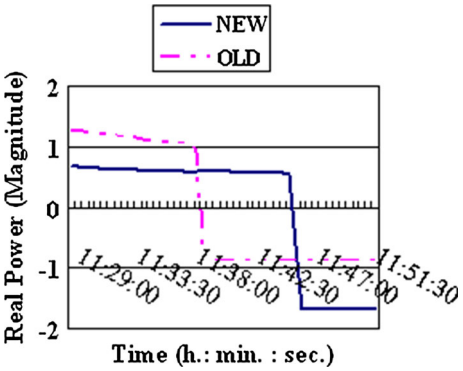

Fig. 10 Load analyses of an electric rice cooker during state transition

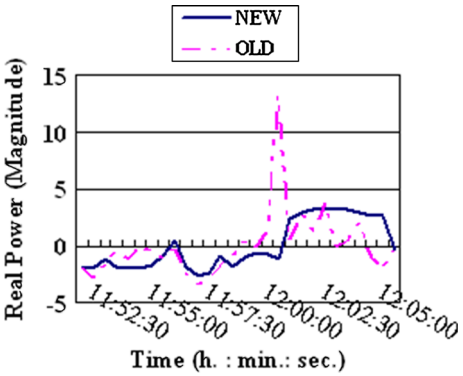

Fig. 11 Load analyses of an electric rice cooker during warming operation

For the aging load in case study 2, the aging load of the appliances can be identified by the proposed method for steady-state P and $PV_{THD}I_{THD}$. It is investigated that the aging load is relevant to internal resistance of the electric appliance from the results. From the results of case study 2, the internal resistance of the electric appliance will be decreased and the P will be increased because of aging load. However, it is very dangerous to increase persistently P of the electric appliance because of aging load. The heat will be increased to damage the insulation of electric wire when the P is more than rated P of the electric appliance for a long time. Accordingly, a fire accident could be happened.

It is interested to evaluate economic beneficial results for aging load. For example, the differences of average power between an old electric rice cooker and a new electric rice cooker in steaming and warming operations are 25.8214 and 1.6926 W, respectively. The total energy consumptions of an old electric rice cooker are more 25.6052 Wh than that of a new one in 0.5 h steaming and 7.5 h warming operations for each day. The total wasted energy will be 9.346 kWh and the lost cost will be 1.082 USD in one year if the price of electricity is averagely 0.11573 USD for an ordinary residential building in American. Moreover, the wasted cost of an old refrigerator will be several ten times than that of a new one.

Accordingly, it is very astonishing to every resident that large amounts of energy consumption and cost were wasted for all old electric appliances.

5 Conclusion

The results of analyses for EMIS can identify load state transition and aging load of intelligent buildings and to know the conditions of loads. The users of building can be reminded to ensure safety of appliances by these results. Besides, some related policies of saving energy, reducing CO_2, health and safety care for hidden elderly and the efficiency of electric appliances can be established and planed by these results of smart buildings.

Based on experimental results of EMIS, the steady-state PS for ELDR in EMIS can be applied extensively to detect state transition and aging of loads in the smart buildings to avoid the wasted energy consumptions. The data mining system of proposed method are useful and simple tools for making decisions of detecting aging load in EMIS for intelligent buildings.

In the future works, the information techniques of proposed method can be embedded in the non-intrusive energy monitoring and load identification system to integrate with EMIS. The system can use a software design and architecture based on software application as services in SOA or SOAIC to deal with a large volume of data in real time. The EMIS will be a powerful system to manager energy information.

Acknowledgments The authors would like to thank the Ministry of Science and Technology of the Republic of China, Taiwan, for financially supporting this research under Contract No. NSC 102-2221-E-228-002.

References

Aman S, Simmhan Y, Prasanna VK (2013) Energy management systems: state of the art and emerging trends. IEEE Commun Mag 51(1):114–119

Bernstein BS, Brancato EL (1993) Aging of equipment in the electric utilities. IEEE Trans Electr Insul 28(5):866–875

Byun J, Hong I, Kang B, Park S (2011) A smart energy distribution and management system for renewable energy distribution and context-aware services based on user patterns and load forecasting. IEEE Trans Consum Electron 57(2):436–444

Chan SC, Tsui KM, Wu HC, Hou Y, Wu YC, Wu FF (2012) Load price forecasting and managing demand response for smart grids: methodologies and challenges. IEEE Signal Process Mag 29(5):68–85

Chang HH (2012) Non-intrusive demand monitoring and load identification for energy management systems based on transient feature analyses. Energies 5(11):4569–4589

Chao KM, Shah N, Farmer R, Matei A (2012) Energy management system for domestic electrical appliances. Int J Appl Logist 3(4):48–60

Goumas SK, Zervakis ME, Stavrakakis GS (2002) Classification of washing machines vibration signals using discrete wavelet analysis for feature extraction. IEEE Trans Instrum Meas 51(3):497–508

Hellinger E (1909) Neue begründung der theorie quadratischer formen von unendlichvielen veränderlichen. Journal für die reine und angewandte Mathematik (in German) 136:210–271

Hernandez L, Baladron C, Lioret J, Chinarro D, Gomez-Sanz JJ, Cook D (2013) A multi-agent system architecture for smart grid management and forecasting of energy demand in virtual power plants. IEEE Commun Mag 51(1):106–113

Hong YY, Chen BY (2007) Locating switched capacitor using wavelet transform and hybrid principal component analysis network. IEEE Trans Power Del 22(2):1145–1152

Hooke JH, Landry BJ, Hart DMA (2004) Energy management information systems: achieving improved energy efficiency: a handbook for managers, engineers and operational staff. Office of Energy Efficiency of Natural Resources Canada, Ottawa

Hou Z, Lian Z, Yao Y, Yuan X (2006) Data mining based sensor fault diagnosis and validation for building air conditioning system. Energy Convers Manag 47:2479–2490

Huber N, Hoorn AV, Koziolek A, Brosig F, Kounev S (2014) Modeling run-time adaptation at the system architecture level in dynamic service-oriented environments. SOCA 8(3):73–89

Huergo RS, Pires PF, Delicato FC, Costa B, Cavalcante E, Batista T (2014) A systematic survey of service identification methods. SOCA 8(3):199–219

Lall P, Hande M, Bhat C, Lee J (2011) Prognostics health monitoring (PHM) for prior damage assessment in electronics equipment under thermo-mechanical loads. IEEE Trans Compon Packaging Manuf Technol 1(11):1774–1789

Lisovich MA, Mulligan DK, Wicker SB (2010) Inferring personal information from demand-response systems. IEEE Secur Priv 8(1):11–20

Nikulin MS (2001) Hellinger distance, Encyclopedia of Mathematics. Hazewinkel, Michiel, Springer. http://www.encyclopediaofmath.org/index.php?title=Hellinger_distance&oldid=16453

Norford LK, Leeb SB (1996) Non-intrusive electrical load monitoring in commercial buildings based on steady-state and transient load-detection algorithms. Energy Build 24(1):51–64

Redpath S, Pocs J (2007) Safety regulations and their impact on microcontrollers in home appliances. In: Paper presented at IEEE IAS annual meeting (IAS 2007), New Orleans, pp 1044–1046

Silva DD, Yu X, Alahakoon D, Holmes G (2011) A data mining framework for electricity consumption analysis from meter data. IEEE Trans Indus Inform 7(3):399–407

Su CL (2011) Load estimation in industrial power systems for expansion planning. IEEE Trans Indus Appl 47(6):2311–2323

Timbus A, Larsson M, Yuen C (2009) Active management of distributed energy resources using standardized communications and modern information technologies. IEEE Trans Indus Electron 56(10):4029–4037

Verdu SV, Garcia MO, Senabre C, Gabaldon A, Garcia Franco FJ (2006) Classification, filtering, and identification of electrical customer load patterns through the use of self-organizing maps. IEEE Trans Power Syst 21(4):1672–1682